Jurnal Ilmu Fisika
Vol. 19, No. 1, March 2027, pp. 11–28
ISSN: 1979-4657 (Print); 2614-7386 (Online)
https://doi.org/10.25077/jif.19.1.11-28.2027

Jurnal Ilmu Fisika
Open Access

Development and Numerical Verification of an Archer Model Radiation Shielding Application for Medical Physics Education

Cindyawati Cindyawati, Yuanita Puspita Dewi Sudarso*

Department of Physics, Faculty of Sciences, Parahyangan Catholic University, Bandung 40141, Indonesia
Research Centre for Applied Science and Instrumentation (RCASI), Parahyangan Catholic University, Bandung 40141, Indonesia

Article Info

Article History:

Received May 16, 2026
Revised October 23, 206
Accepted October 25, 2026
Published online November 01, 2026

Keywords:

radiation shielding
archer model
broad-beam transmission
numerical verification
medical physics education

Corresponding Author:

Yuanita Puspita Dewi Sudarso,
Email: yuanpds@unpar.ac.id

ABSTRACT

Accurate radiation shielding calculations are essential for radiation protection and medical physics education. This study developed and numerically verified an interactive desktop application for broad-beam photon shielding calculations using the Archer transmission model. The application integrates published Monte Carlo-derived fitting parameters for Tc-99m, I-131, F-18, and Lu-177 in lead, concrete, and steel, enabling forward and inverse shielding calculations with buildup effects and selectable weekly design goals of 0.02 mSv/week. Numerical verification was performed by comparing application outputs with independent calculations and published reference data. For the Tc-99m lead shielding example (0.637 mm), the application reproduced the published transmission result, while inverse–forward round-trip calculations achieved a composite target within a relative residual of approximately 5×10^{-16}. Additional comparisons were conducted using published fractional-value layers for nine radionuclide–material combinations. The results demonstrate numerical consistency in the implemented calculations and provide an interactive framework for exploring photon attenuation and shielding thickness in medical physics education. However, Ga-68 calculations remain based on unvalidated F-18 surrogate parameters, and multilayer shielding estimates have not been independently validated against experimental or Monte Carlo reference data. Therefore, the application is intended for educational use rather than clinical shielding design.

Copyright © 2026 Author(s)

1. INTRODUCTION

Ionizing radiation is an integral component of modern nuclear medicine practice and is widely used for the diagnostic imaging and radionuclide therapy. Radionuclides such as Tc-99m for SPECT, F-18 for PET scans, I-131 for thyroid therapy, and Lu-177 for peptide receptor radionuclide therapy contribute substantially to clinical practice (Cherry et al., 2012; Levart et al., 2019; Oumano, 2025; Riveira-Martin et al., 2023). Their use also requires appropriate radiation protection measures, particularly for occupational and public exposure associated with nuclear medicine facilities (Salehzahi & Tse, 2020). The present application focuses on external photon shielding and estimates photon transmission through shielding materials using broad-beam attenuation parameters. The model represents photon emissions associated with the selected radionuclides but does not directly calculate beta-particle transport, beta-induced bremsstrahlung, or patient-specific internal dosimetry. Therefore, its results should be interpreted as photon-shielding estimates rather than a comprehensive assessment of all radiation-protection requirements associated with these radionuclides.

The international system of radiological protection established by the International Commission on Radiological Protection (ICRP) (ICRP, 2007) is based on the principles of justification, optimization

Attribution-NonCommercial 4.0 International

of protection, and dose limit. In planned exposure situations, dose limits apply to occupational and public exposure, whereas medical exposure of patients is subject to a different framework based on justification and optimization and is not governed by the same dose limits. In nuclear medicine facilities, appropriate shielding design is an important measure for optimizing protection against external radiation exposure, particularly for workers and members of the public. Reliable shielding estimates require consideration of photon attenuation and the contribution of scattered radiation, which can be represented by a buildup factor in broad-beam calculations.

In medical physics education, understanding photon attenuation, scattered radiation, and buildup effects is important for interpreting practical shielding calculations. Conventional half-value layer (HVL) data can provide a useful description of attenuation under specified beam and measurement conditions (Prasada & Azzi, 2025). However, narrow-beam attenuation data should not be used directly as a substitute for broad-beam transmission estimates when scattered radiation contributes to the radiation field behind a shielding barrier. The use of the Archer equation provides a way to represent broad-beam photon transmission and calculate the shielding thickness required for a specified transmission target (Paixão et al., 2025) . From an instructional perspective, translating this equation into an interactive application may help learners explore the relationship between barrier thickness, material properties, transmission, and the selected design target. The present study introduces such an application as a supplementary educational resource; it does not assess student difficulties or demonstrate improvements in learning outcomes.

Several approaches have been developed to describe photon transmission through shielding barriers under broad-beam conditions. The three-parameter Archer equation represents the transmission factor as a function of shielding thickness using the fitting parameters α, β, and γ (Archer et al., 1983). The equation can be evaluated in the forward direction to estimate transmission for a specified thickness and inverted to estimate the thickness required for a target transmission. For nuclear medicine applications, the applicability of the fitted parameters depends on the radionuclide emission data, the modeled radiation field, the shielding material, and the conditions used to generate the underlying transmission data. The radionuclide-specific parameters reported by (Oumano et al., 2025) are therefore used here within the scope of the photon-transmission model described in that study. They should not be interpreted as universal parameters for arbitrary monoenergetic beams or radiation geometries. Although the Archer equation is compact, its forward and inverse forms can be cumbersome to evaluate repeatedly by hand. The application developed in this study integrates these calculations into a graphical user interface, allowing users to examine the relationship between shielding thickness, photon transmission, and material selection.

Previous studies have established theoretical and computational approaches for evaluating photon attenuation, radiation buildup, and shielding performance. Shimizu et al. (2004) developed gamma-ray buildup-factor data, while Manohara et al. (2011) investigated energy-absorption buildup factors for biological materials. More recently, Oumano et al. (2025) reported Monte Carlo-derived broad-beam transmission factors and Archer fitting parameters for radionuclides commonly used in nuclear medicine, providing a quantitative basis for shielding calculations (Wu et al., 2025). Existing computational tools, including Phy-X/PSD and software developed for radiotherapy and diagnostic X-ray facilities, have also demonstrated the applicability of computer-based shielding calculations (Şakar et al., 2020; Mann & Mann, 2021). Nevertheless, these studies address different computational objectives and do not, by themselves, establish the numerical reliability of the application developed in the present work. Recent work has further examined shielding-method comparisons for nuclear medicine, including I-131 isolation-room design (Gonzales et al., 2025), and Archer-type transmission fitting for diagnostic imaging beams (Li et al., 2024). More sophisticated three-dimensional shielding tools address geometry-dependent and multilayer effects, as demonstrated by POKER (Chen et al., 2025), while new Monte Carlo buildup-factor calculations investigate the dependence on geometry and penetration depth (Sun et al., 2025).

The present study addresses the implementation and numerical verification of radionuclide-specific Archer transmission calculations within an interactive educational application. Particular attention is given to the consistency of forward and inverse calculations, agreement with published

reference values, and the explicit identification of limitations associated with surrogate radionuclide parameters and approximate multilayer shielding calculations. Unlike studies focused primarily on generating attenuation parameters or developing shielding models, this work examines the reproducibility of established calculations within a desktop graphical user interface. Its contribution lies in combining numerical verification with interactive exploration of shielding parameters for medical physics education, without claiming the development of a new physical model or experimentally validated clinical shielding tool. Contemporary tools such as GRASP-X and PARSO demonstrate the continuing development of accessible computational shielding environments (Bektasoglu & Bayraktar, 2026; Tarabin & Hisseine, 2026). Accordingly, the contribution claimed here is limited to the implementation and numerical checking of the specific Archer calculation workflow rather than the general invention of radiation-shielding software (Hansda & Mammen, 2021).

Advances in computer simulation technology have created opportunities to develop interactive learning tools capable of bridging the gap between theory and practice (Chau et al., 2022). Python-based simulations with graphical user interfaces (GUI) enable students to visually and intuitively explore the relationships among material parameters (α, β, γ), shielding thickness, and attenuation effectiveness (Ganou et al., 2023; Sosa Vera & Andres, 2022). Recent studies of interactive radiological education describe cloud-based CT practice and problem-based learning approaches (Chau & Arruzza, 2023; Arruzza et al., 2023); these provide an educational rationale but do not establish learning gains for the present application.

This study aims to develop a radiation shielding calculation application with a user-friendly graphical interface for medical physics education. The application implements the published Archer broad-beam transmission model using radionuclide-specific fitting parameters for five radioisotopes, with the F-18 parameter set used as an unvalidated surrogate for Ga-68. The software contributions include forward and inverse shielding calculations, interactive attenuation-curve visualization, material comparison, and occupancy-factor and dose-limit inputs. Two-layer composite shielding is implemented using an independent-layer approximation and has not been validated as an extension of the original Archer model. The novelty of this study lies primarily in integrating these functions into an interactive desktop application for educational use, rather than in developing a new attenuation equation or validating a new shielding model.

The application is expected to serve as a learning tool that helps students understand the influence of the α, β, and γ parameters on shielding effectiveness, compare the performance of various materials at different photon energies, explore composite shielding designs, and relate theoretical concepts to practical scenarios in nuclear medicine facilities.

2. METHOD

2.1 Mathematical Model for Radiation Shielding Calculations

The application estimates photon transmission through shielding materials using the three-parameter Archer equation fitted to broad-beam transmission data. The Archer equation is used to calculate the transmission factor (B) for a specified shielding thickness and to estimate the thickness required to achieve a target transmission.:

$$B = \left[\left(1 + \frac{\beta}{\alpha}\right) e^{\alpha\gamma x} - \frac{\beta}{\alpha}\right]^{-\frac{1}{\gamma}} \quad (1)$$

The required shielding thickness for a specified target transmission factor is determined by rearranging the Archer equation, as given in Equation (2)

$$x = \frac{1}{\alpha\gamma} \ln\left(\frac{{B_{target}}^{-\gamma} + \frac{\beta}{\alpha}}{1 + \frac{\beta}{\alpha}}\right) \quad (2)$$

The parameters α and β are empirical Archer fitting parameters with units of inverse length, whereas γ is dimensionless. These parameters describe the fitted relationship between shielding thickness and photon transmission and are not independent physical measures of the buildup factor (Basu et al., 2019).

For a two-layer composite material, the total transmission factor is calculated as the product of the individual transmission factors:

$$B_{total} \approx B_1 \times \mathrm{B}_2 \tag{3}$$

where B_1 and B_2 are the transmission factors assigned to the individual layers. This approximation has not been validated for heterogeneous shielding configurations and does not explicitly account for changes in the photon spectrum or scattering at the interface between materials.

Table 1. Types of radioisotopes along with the energies used in the simulation.

Radioisotope	Energy (keV)	Γ (mSv.m^2.GBq^{-1}.h^{-1})	Clinical Application
Tc-99m	140	0.022	SPECT imaging
I-131	364	0.052	Thyroid therapy
F-18	511	0.135	PET imaging
Ga-68	511	0.140	PET imaging
Lu-177	208	0.008	Peptide radiotherapy

Table 2. Archer fitting parameters for different material–energy combinations.

Isotope	Material	α (mm^{-1})	B (mm^{-1})	γ
Tc-99m	Lead	2.558	1.010	4.344
	Low-density concrete	0.02047	−0.01122	0.4389
	High-density concrete	0.03102	−0.01729	0.3622
	Steel	0.1581	−0.04346	0.2602
Lu-177	Lead	0.3855	1.071	0.2822
	Low-density concrete	0.01615	−0.007056	0.5194
	High-density concrete	0.02477	−0.01173	0.4404
	Steel	0.0797	2.243	28.74
I-131	Lead	0.1082	0.2072	0.5385
	Low-density concrete	0.01363	−0.007896	0.4847
	High-density concrete	0.02062	−0.01220	0.4179
	Steel	0.05786	−0.02574	0.8742
F-18 and Ga-68	Lead	0.166	−0.02184	0.2436
	Low-density concrete	0.01126	−0.006463	0.7475
	High-density concrete	0.01558	−0.008775	0.8600
	Steel	0.05032	−0.02632	1.223

2.2 Material and Radioisotope Parameters

The application uses Archer fitting parameters for five radionuclides listed in Table 1. Although F-18 and Ga-68 both emit 511 keV annihilation photons, their dose-rate constants differ. F-18 parameters are used as an unvalidated surrogate for Ga-68, without assuming equivalence in their emission spectra or shielding characteristics.

Table 3 Physical properties and elemental compositions of shielding materials used in the simulation.

Material	Reference	Density (g/cm^3)	Elemental Composition (Mass Fraction)
Low Density Concrete	(Ferrari et al., 2005)	1.6	Hydrogen (0.01), Carbon (0.001), Oxygen (0.529107), Sodium (0.016), Magnesium (0.002
High Density	(Ferrari et al., 2005)	2.3	Aluminum (0.033872), Silicon (0.337021), Potassium (0.013), Calcium (0.044), Iron (0.014
Steel	(AZoM, 2012)	7.85	Iron (0.97), Manganese (0.0095), Chromium (0.0065), Silicon (0.006), Molybdenum (0.0023), Carbon (0.004675), Zirconium (0.001), Boron (0.000025)
Lead	(Hubbell & Seltzer, 1995)	11.35	Lead (1.000000)

The Archer fitting parameters, adopted from the Monte Carlo-based broad-beam transmission data reported by Oumano et al. (2025), are presented in Table 2, while the material densities and elemental compositions are listed in Table 3. The applicability of these parameters is limited to the thickness and transmission ranges established in the source study.

2.3 Dose Calculation

For a point source with activity (A) (GBq) located at a distance (d) (m) from the dose evaluation point, the unshielded dose rate is calculated using the radionuclide-specific dose-rate constant (Γ) (mSv m^2 GBq^{-1} h^{-1}), as follows:

$$\dot{D_0} = \frac{\Gamma A}{d^2} \tag{4}$$

The unshielded weekly dose, (D_0) (mSv/week), is then estimated as

$$D_0 = \dot{D_0} t O \tag{5}$$

where t is the exposure duration (h/week) and (O) is the occupancy factor (dimensionless). The activity is assumed to remain constant during the specified exposure period. Radioactive decay during exposure, patient self-attenuation, and additional contributions from scattered radiation are not explicitly modeled. The source is approximated as a point source, and the inverse-square law is applied using the distance from the source to the dose evaluation point.

Occupancy factors of 1, 0.2, 0.05, and 0.025 are assigned to offices, corridors, toilets/storage rooms, and outdoor areas, respectively, based on the occupancy categories recommended in NCRP Report No. 147 (NCRP, 2004). These values are adopted as representative design assumptions. Actual occupancy and room use may require different values.

For this application, a weekly dose design goal (P) of 0.02 mSv/week is assumed for areas accessible to members of the public. For an assumed 50-week working year, this corresponds arithmetically to 1 mSv/year. This value is used as a computational design target and is not presented as

a universal weekly regulatory dose limit. Applicable public and occupational dose limits must be assessed separately in accordance with the relevant radiation-protection regulations.

If the estimated unshielded weekly dose exceeds the selected design goal, the target transmission factor is calculated as

$$B_{\text{target}} = \frac{P}{D_0} \tag{6}$$

The required shielding thickness is then calculated using the inverse Archer equation (Equation 1) with the corresponding fitting parameters for the selected material and photon energy. The transmission factor at the calculated thickness is evaluated using the Archer equation (Equation (2)), and the estimated weekly dose behind the barrier is calculated as $D_{shield} = D_0 B$. If $D_0 \leq P$, no additional shielding is indicated to meet the selected design goal under the specified assumptions. However, this result represents a preliminary estimate and does not, by itself, demonstrate that the shielding is adequate for an actual facility.

2.4 Simulation Implementation

The application was developed using Python 3.8, with Tkinter for the graphical user interface, NumPy for numerical computation, and Matplotlib for visualization. The complete Python source code, including the calculation module and GUI scripts, is publicly available on (https://github.com/cindyawati633/Shielding-Calculation.git). The software version used to generate the results reported in this study was Python 3.12, with the code developed and executed using Visual Studio Code (VS Code). The repository includes installation instructions, dependency versions, information the supported operating system, the software licence, and an example demonstrating how to run the application. The current version is a locally executed desktop application and is not hosted online. Development of a web-based version using a framework such as Streamlit or Dash is planned for future work.

The application architecture consists of three main modules:

a. Calculation Module: Implements the Archer equation to calculate the transmission factor as a function of shielding thickness and uses the inverse Archer equation to determine the required thickness analytically. Numerical safeguards are included to handle extreme values during transmission-factor evaluation.
b. Interface Module: Provides input panels for source parameters (activity, distance, and workload), material selection, and occupancy factors. The output panel displays numerical calculation results and real-time attenuation curve graphs.
c. Visualization Module: Generates plots of estimated dose versus shielding thickness and indicates the calculated thickness required to meet the selected design goal. The application uses 0.02 mSv/week as an assumed computational design target for public-access areas, rather than treating it as a universal weekly regulatory dose limit.

For numerical stability, the current implementation bounds the calculated transmission factor (B), between 10^{-10} and 100 and returns a lower-bound value of 10^{-10} under certain extreme or invalid numerical conditions. This safeguard can truncate the calculated transmission factor and cause the reported value to differ from the unbounded mathematical result. It does not validate the Archer model outside the range of the underlying fitting data. Therefore, numerical safeguards must be distinguished from physical-model validity, and results near the imposed bounds or outside the applicable fitting range should be treated with caution.

The clamping procedure is implemented as a numerical safeguard to prevent numerical underflow and overflow during transmission-factor evaluation. When the calculated transmission factor falls below the imposed lower bound of 10^{-10}, it is set to this minimum value. Consequently, the evaluated transmission may be higher than the corresponding unbounded mathematical result, introducing a numerical bias toward overestimating transmission under extreme attenuation conditions. Furthermore, once the lower bound is reached, further increases in shielding thickness may no longer produce changes in the reported transmission factor, resulting in a numerical truncation artifact. These effects are numerical limitations rather than physical corrections to the radiation transport model.

Therefore, results for very thick shielding barriers should be interpreted with caution, particularly when the calculated transmission factor approaches the imposed lower bound.

A numerical boundary test was performed using the Archer parameters for Tc-99m and lead α = 2.558, β =1.010, and γ = 4.344. For an input thickness parameter of (x = 9), the calculated transmission factor before clamping was approximately 9.3×10^{-10}, which was replaced by the imposed lower bound of 10^{-10}. This represents an approximately 7.5% increase in the reported transmission factor. At (x = 10), the unbounded value was approximately 7.2×10^{-12}, but the reported value remained at 10, demonstrating numerical truncation. These tests illustrate the effect of the numerical floor and do not establish model validity below the applicable fitting range of $B \leq 10^{-3}$.

2.5 Validation and Verification

The numerical implementation was verified in three steps. First, the results were compared with manual calculations using Equations (3) and (4). For the standard Tc-99m lead shielding scenario, The unshielded weekly dose was calculated as $D_0 = (0.022 \times 0.5)/(40 \times 2^2) = 0.11$ mSv/week. With a weekly design goal of 0.02 mSv/week, the target transmission factor was $B = 0.02/0.11 = 0.182$, corresponding to a calculated lead thickness of x = 0.637 mm, which was reproduced by the application. Second, the thickness obtained from the inverse Archer equation was substituted into the forward equation to verify that the target transmission was recovered (round-trip check). Third, the calculated thicknesses for transmission factors of 0.5, 0.25, 0.1, 0.01, and 0.001 were compared with the fractional-value layers reported by Oumano et al. (2025). These comparisons confirm the numerical consistency of the implementation but do not independently validate the physical accuracy of the underlying Archer model.

However, this comparison does not constitute an independent validation of the physical accuracy of the model. In particular, the composite shielding approximation for the lead–concrete configuration has not yet been independently validated against Monte Carlo simulations.

The evaluation in this study focused on numerical verification of the application rather than user-based evaluation. No medical physics students were recruited as respondents, and no questionnaire or user-evaluation instrument was administered. Accordingly, the usability, user experience, and learning effectiveness of the application are untested. Because this paper describes the development and numerical verification of the software, a student study was considered outside its scope.

3. RESULTS AND DISCUSSION

3.1 Characteristics of the Simulation Application

The application was developed with a three-panel interface (Figure 1). The input panel allows users to select radionuclides (Tc-99m, I-131, F-18, Lu-177, and Ga-68), shielding materials (lead, low- and high-density concrete, and steel), and scenario parameters, including activity (0.1–10 GBq), distance (0.5–10 m), workload (1–168 hours/week), and occupancy factor (0.025–1.0). The results panel displays the calculated dose rate, potential weekly dose, required shielding thickness, and transmission factor. The graph panel presents dose-versus-thickness curves, with markers indicating the required shielding thickness and the applicable dose limit.

As an illustrative example, radiation shielding calculations can be compared using the radioisotopes Technetium-99m (Tc-99m) and Fluorine-18 (F-18). These two isotopes were selected because they possess different photon energy characteristics and clinical applications, thereby providing a representative overview of the influence of radiation energy on the transmission factor, buildup factor, and the required shielding material thickness.

Based on the simulation results using a standard parameter scenario (activity: 0.5 GBq, distance: 2 m, workload: 40 hours/week, occupancy factor (O = 1)), significant variations in the required shielding thickness were observed among different materials and photon energies. In Figure 2, the required lead (Pb) thickness to reduce the Tc-99m dose to the safe limit was found to be 0.6 mm. In contrast, Figure 3 shows that a lead (Pb) thickness of 23.3 mm was required to reduce the F-18 dose to the safe limit. These values are scenario-specific results of the model for the stated inputs and should not be interpreted as universally safe barrier thicknesses.

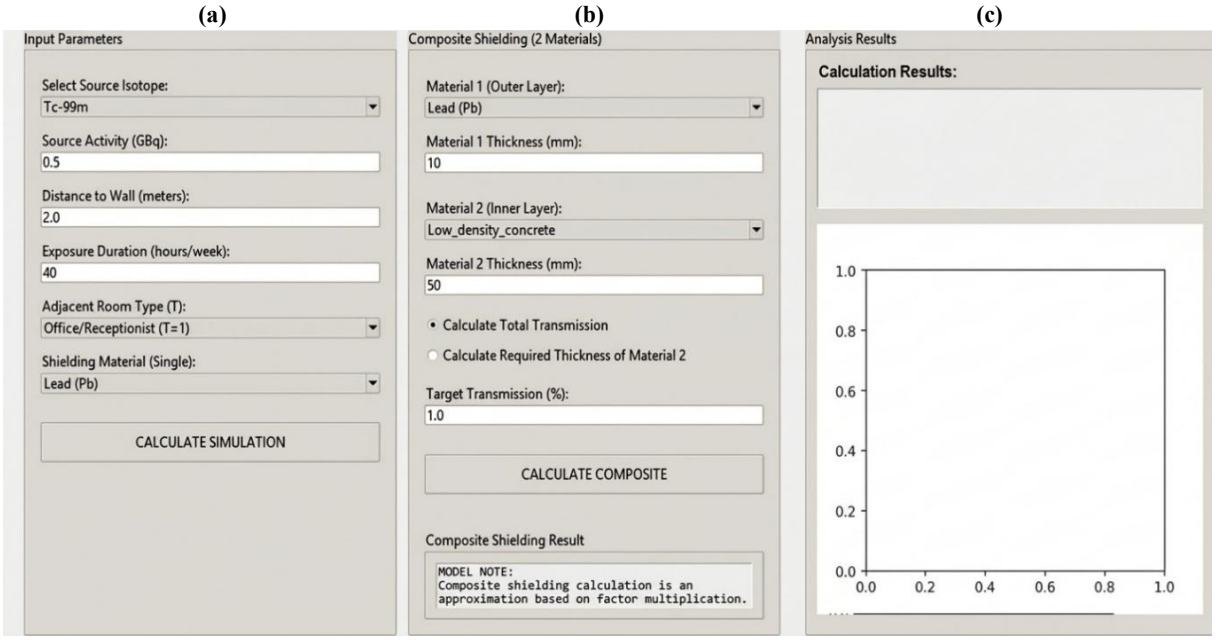


Figure 1. Graphical user interface of the developed radiation shielding calculator: (a) radionuclide, exposure, and shielding inputs; (b) composite shielding configuration and calculation settings; and (c) calculated results and photon transmission visualization.

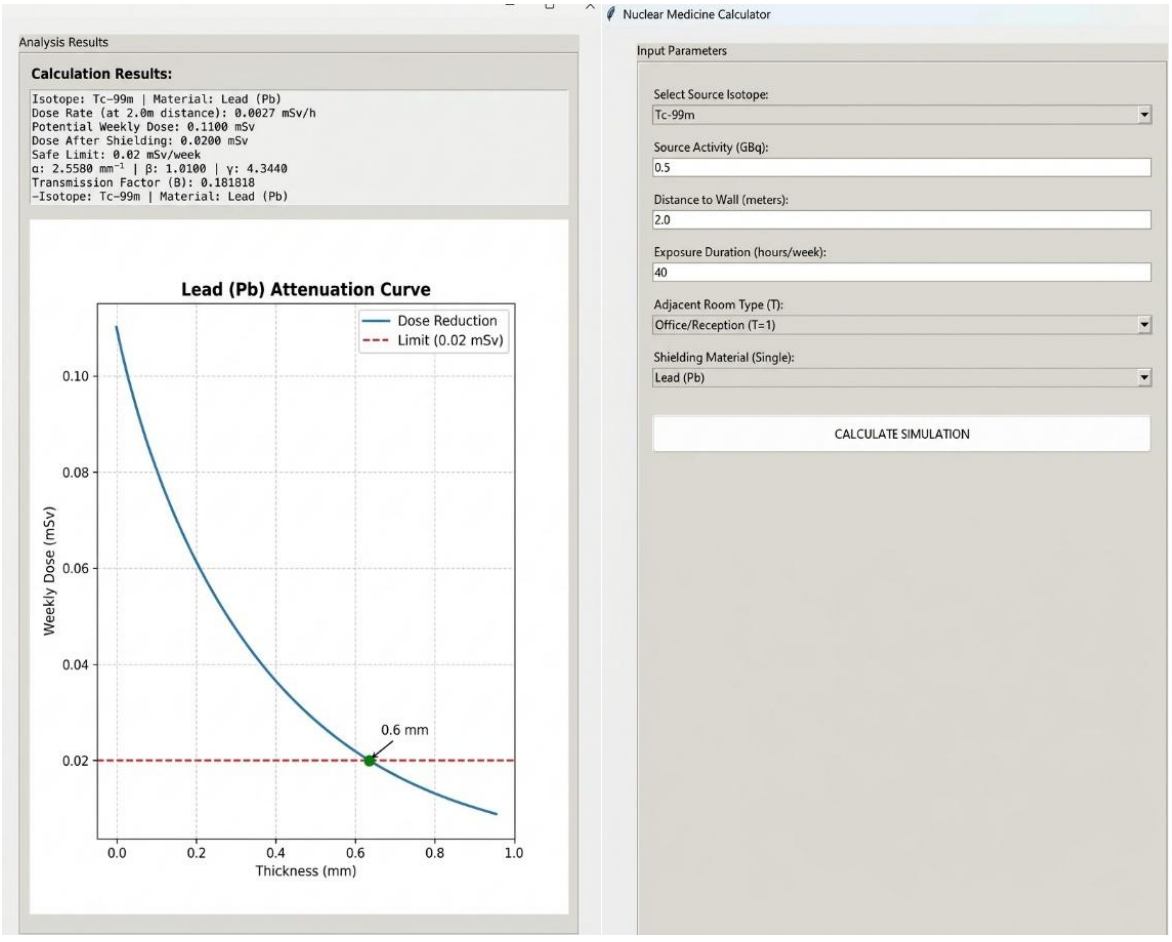


Figure 2. Dose attenuation curve for a Tc-99m source (0.5 GBq, 2 m, 40 h/week, $O = 1$) through a lead (Pb) barrier. The red dashed line indicates the weekly design goal (0.02 mSv/week), while the green marker shows the required Pb thickness (0.64 mm) to reduce the unshielded dose (0.11 mSv/week) to this level

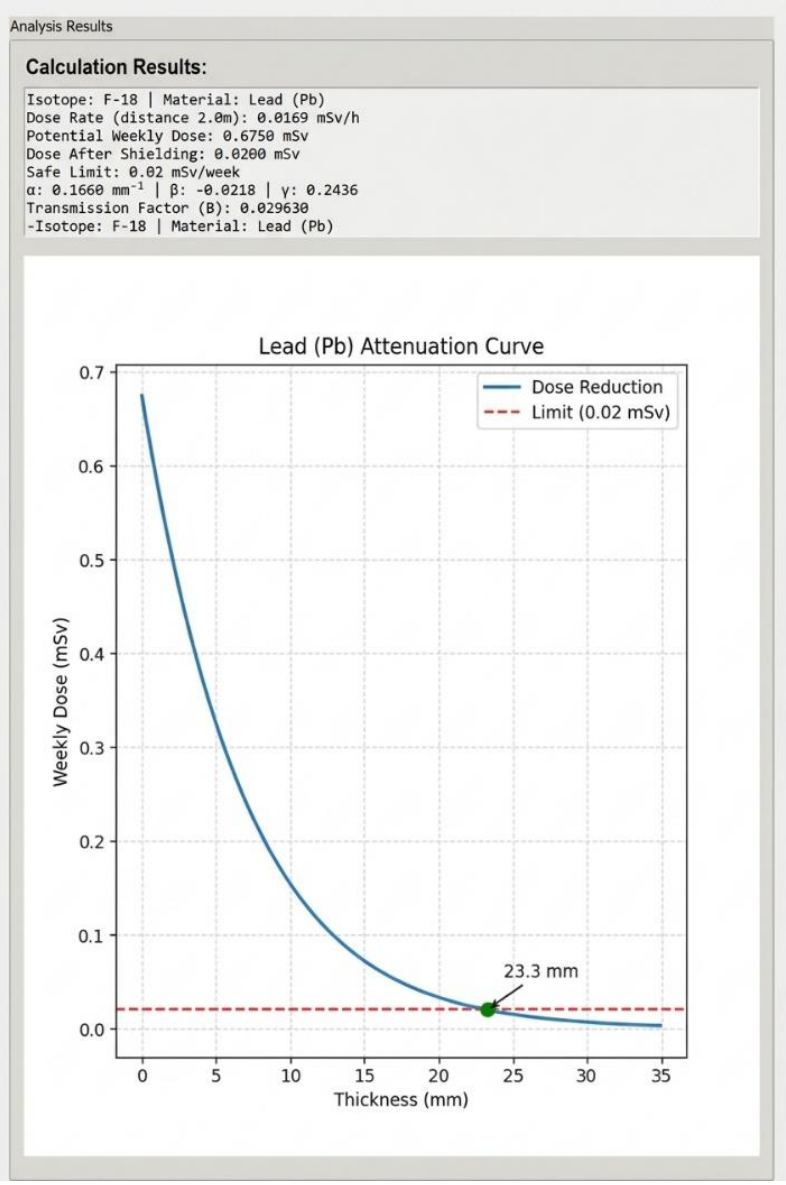


Figure 3. Dose attenuation curve for an F-18 source (0.5 GBq, 2 m, 40 h/week, O = 1) through a lead (Pb) barrier using the Archer model. The red dashed line indicates the weekly design goal (0.02 mSv/week), while the green marker shows the required Pb thickness (23.3 mm) to reduce the unshielded dose (0.675 mSv/week) to this level

The results show that F-18 requires substantially thicker lead shielding (23.3 mm) than Tc-99m (0.64 mm) under the same exposure conditions. This difference reflects the combined effects of photon energy, radionuclide-specific dose-rate constants, and Archer fitting parameters on the calculated shielding requirements.

3.2 Comparison of Materials at Different Energies

Simulations under a standard scenario (activity: 0.5 GBq, distance: 2 m, workload: 40 hours/week, occupancy factor O =1) demonstrated significant variations in the required shielding thickness among different materials and radionuclides. The calculated thicknesses are scenario-specific. They differ between the two radionuclides because of combined factors: the dose-rate constant Γ, which sets the unshielded dose and hence the target B, and the parameters (α, β, γ), which differ for each material–radionuclide combination.

Table 4. Calculated thicknesses (mm) for the standard scenario (0.5 GBq, 2 m, 40 h/week, $O = 1$, $P = 0.02$ mSv/week)

Radionuclide	Γ	Unshielded weekly dose	Target (B)	Pb	Steel	High-density concrete	Low-density concrete
Tc-99m	0.022	0.110	0.1818	0.64	13.9	95.7	138.3
F-18	0.135	0.675	0.0296	23.3	81.8	285.6	408.9

In this two-radionuclide example, the thicknesses calculated for the standard scenario are larger for F-18 (511 keV) than for Tc-99m (140 keV) in all four materials (Table 4). This comparison cannot be interpreted as an effect of photon energy alone, because the two cases differ in the target transmission (through Γ) and in the Archer parameters. The general tendency for higher-energy photons to be attenuated less per unit thickness (Marshall et al., 2025; Saleh et al., 2021) is consistent with this direction, but it should not be extrapolated to all photon energies, since attenuation depends on photon energy, material composition, and the dominant interaction regime. The relationship between photon energy and shielding thickness is non-linear due to the influence of different Archer parameters. For Tc-99m in lead, the high value of $\alpha = 2.558$ mm^{-1} indicates highly effective attenuation. In contrast, for F-18 with a low value of $\alpha = 0.166$ mm^{-1}, deeper penetration occurs, requiring substantially greater material thickness for adequate shielding. However, α alone does not determine the required thickness, because β and γ also shape the curve. The relationship between photon energy and shielding thickness is non-linear due to the influence of different Archer parameters. For Tc-99m in lead, the high value of $\alpha = 2.558$mm^{-1} indicates highly effective attenuation. In contrast, for F-18 with a low value of $\alpha = 0.166$mm^{-1}, deeper penetration occurs, requiring substantially greater material thickness for adequate shielding.3.3 Visualization of Attenuation Curves Other recent approaches include neural-network-assisted shielding optimization, which illustrates an alternative computational objective rather than a validation of the Archer model (Dorostkar & Rasouli, 2025).

The attenuation curve graphs generated by this simulation application provide valuable pedagogical insights, particularly in visualizing the dynamics of radiation interactions with shielding materials. The attenuation-curve display of the application shows the transmission predicted by the fitted Archer function as a function of barrier thickness (Figures 2 and 3). Because α, β, and γ are empirical fitting parameters, the curves are interpreted here as fitted transmission curves. Their shape does not, by itself, quantify a buildup contribution or identify the scattering history of photons in the barrier, and no comparison with pure exponential attenuation is presented. The curve shape thus depends on the material–radionuclide combination, and users can explore this dependence by changing the material and radionuclide in the application.

The attenuation-curve behavior depends on the material–energy combination represented by the Archer fitting parameters. In the present results, lead exhibits a positive β value for some photon energies, whereas concrete generally exhibits negative β values. These differences affect the shape of the fitted transmission curves relative to the corresponding exponential attenuation behavior. However, β should be interpreted as an empirical fitting parameter within the Archer equation rather than as a direct, independent measure of the amount of scattered radiation (Sun et al., 2026). Its physical interpretation should therefore consider the complete equation and the corresponding material–energy parameters.

For lead (Pb), the positive β value reported for Tc-99m ($\beta = 1.010$) affects the initial slope and curvature of the fitted Archer transmission function. However, β is an empirical fitting parameter, and its positive sign alone does not quantify the buildup factor or establish the magnitude of scattered radiation. The attenuation behavior should therefore be interpreted using the complete Archer equation and the corresponding material–energy parameters.

The role of β in shaping the Archer transmission curve can be examined by defining the dimensionless auxiliary term N, where $B = N^{(-1/\gamma)}$. The auxiliary term is expressed as

$$\boldsymbol{N = \left(1 + \frac{\beta}{\alpha}\right) e^{(\alpha\gamma x)} - \frac{\beta}{\alpha}} \tag{7}$$

The logarithmic attenuation rate is then calculated as

$$\frac{-d(\ln B)}{dx} = (\alpha + \beta)e^{\frac{\alpha\gamma x}{N}} \quad (8)$$

This relationship is valid for $\alpha + \beta > 0$, a condition satisfied by all parameter combinations in Table 2. At $x = 0$, $N = 1$ and the attenuation rate equals $\alpha + \beta$; as x increases, the rate approaches α. The product $\alpha\gamma$ determines the characteristic thickness scale of this transition. These expressions describe the fitted mathematical model and do not independently quantify the physical buildup contribution.

The sign of β also depends on on the material–energy combination. In Table 2, lead has a positive β at 140, 208, and 364 keV (Tc-99m: 1.010 mm^{-1}; Lu-177: 1.071 mm^{-1}; I-131: 0.2072 mm^{-1}) but a slightly negative β at 511 keV (-0.02184) mm^{-1}. The material-dependent behavior of β is therefore a property of the material–energy combination rather than of the material alone, which is a useful point for students to explore with the application.

The application is an educational model with stated assumptions: a point source in air, an infinite barrier at normal incidence, no room scatter from ceilings and floors, no patient self-attenuation or radioactive decay during exposure, a selected weekly design goal, the F-18 parameter set as an unvalidated surrogate for Ga-68, and an independent-layer product approximation for composite shielding that has not been validated against Monte Carlo simulations. Its outputs are preliminary estimates under these assumptions and do not demonstrate that a barrier is safe or complies with radiation protection standards or regulations. Actual facility shielding design requires a qualified medical physicist or radiation protection expert and an assessment against applicable regulatory requirements.

3.4 Effectiveness of Composite Shielding

Composite shielding, which combines two or more materials, can be used to attenuate radiation while balancing shielding performance, structural weight, and cost. In this study, a combination of lead (Pb) as Material 1 and high-density concrete as Material 2 was evaluated for the attenuation of radiation from the F-18 isotope. Two scenarios were investigated: (1) calculating the total transmission for specified thicknesses of both materials and (2) determining the required thickness of the second material to achieve a specified transmission target. The total transmission was approximated by multiplying the transmission factors calculated independently for the two materials. This approach provides a first-order estimate and does not explicitly account for changes in the photon energy spectrum, secondary photon production, or the effects of material-layer ordering, and it has not been benchmarked against Monte Carlo simulations; the composite results below are therefore preliminary estimates.

3.4.1 Total Transmission Calculation Results for a Fixed Composite Design

Based on Figure 4, the composite shielding simulation for F-18 using a combination of 10 mm Pb and 50 mm high-density concrete produced a lead transmission factor (B_1) of 0.2284 (22.84%), a high-density concrete transmission factor (B_2) of 0.6669 (66.69%), and a total transmission factor B_{total} ($B_1 \times B_2$) of 0.1524 (15.24%). Figure 4 illustrates the predicted composite transmission for fixed layer thicknesses.

A total transmission value of approximately 15.24% is equivalent to the use of 12.67 mm of pure Pb shielding. Based on the application's selected 5% transmission criterion, this configuration does not meet the specified target because the calculated total transmission remains approximately 15.24%. The 5% value is an illustrative threshold used in the application to classify results, not a universal adequacy criterion. However, from a practical perspective, the total thickness of 60.0 mm represents a design that is relatively easy to implement, may require limited space, and may not excessively burden the building structure; these considerations are untested, as no cost, area, or structural-loading calculations were performed. This result indicates that for high-energy radiation such as F-18, the addition of 50 mm of concrete behind 10 mm of Pb is still inadequate to achieve optimal radiation attenuation.

3.4.2 Optimization of Material Thickness Based on Target Transmission

At the subsequent evaluation stage, the simulation approach is focused on designing shielding specifications that precisely satisfy radiation safety standards. In this optimization scenario, the target transmission limit is strictly set at 1.0%. This is a chosen target for illustration, not a radiation safety standard. It is stricter than the 5% level used in the preceding example, which the 15.24% total transmission did not reach. The composite configuration retains the same base materials, where a 10 mm lead (Pb) layer serves as the primary shielding material with an initial transmission factor (B_1) of 0.228479. The thickness of the secondary material, high-density concrete, is then computationally determined to accommodate the remaining required attenuation.We The calculation does not minimise total thickness, mass, or cost.

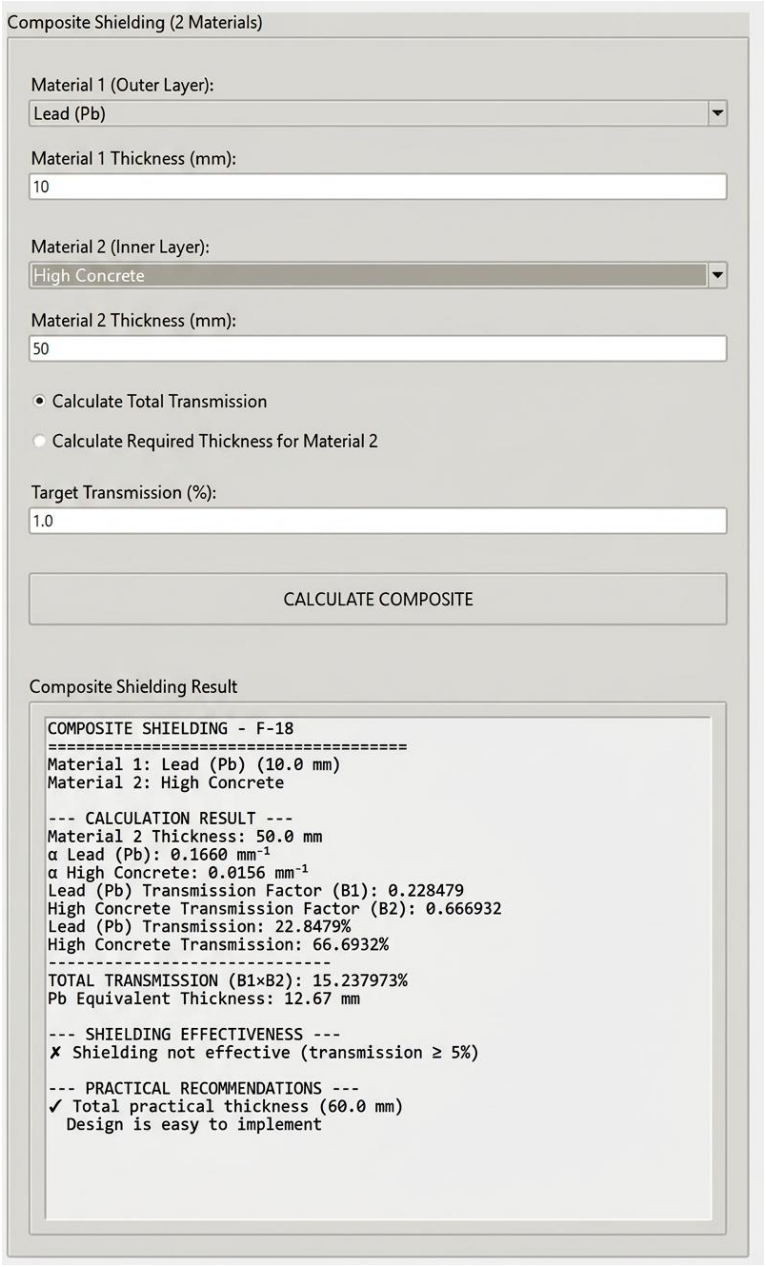


Figure 4. Total photon transmission through composite shielding of lead (10 mm) and high-density concrete (50 mm) for an F-18 source. Individual transmission factors are $B_1 = 0.2285$ and $B_2 = 0.6669$, yielding $B_{total} = 0.1524$ (15.24%). The independent-layer approximation neglects layer-order effects, spectral changes, and secondary radiation

Based on the computational results, achieving the 1% total transmission target requires a concrete-layer transmission factor of $B_{2target} = B_{target} / B_1 = 0.01 / 0.228479 = 0.043768$. Using the Archer fitting parameters for high-density concrete at 511 keV ($\alpha = 0.01558$ mm^{-1}, $\beta = -0.008775$ mm^{-1}, and $\gamma = 0.8600$), the calculated concrete thickness is 259.74 mm. Substituting this thickness into the forward Archer equation yields a total transmission of 1.0%, with a relative residual of $|B_{total} - B_{target}| / B_{target} \approx 5 \times 10^{-16}$. This round-trip check confirms the numerical consistency of the forward and inverse calculations but does not independently validate the physical accuracy of the composite shielding approximation.

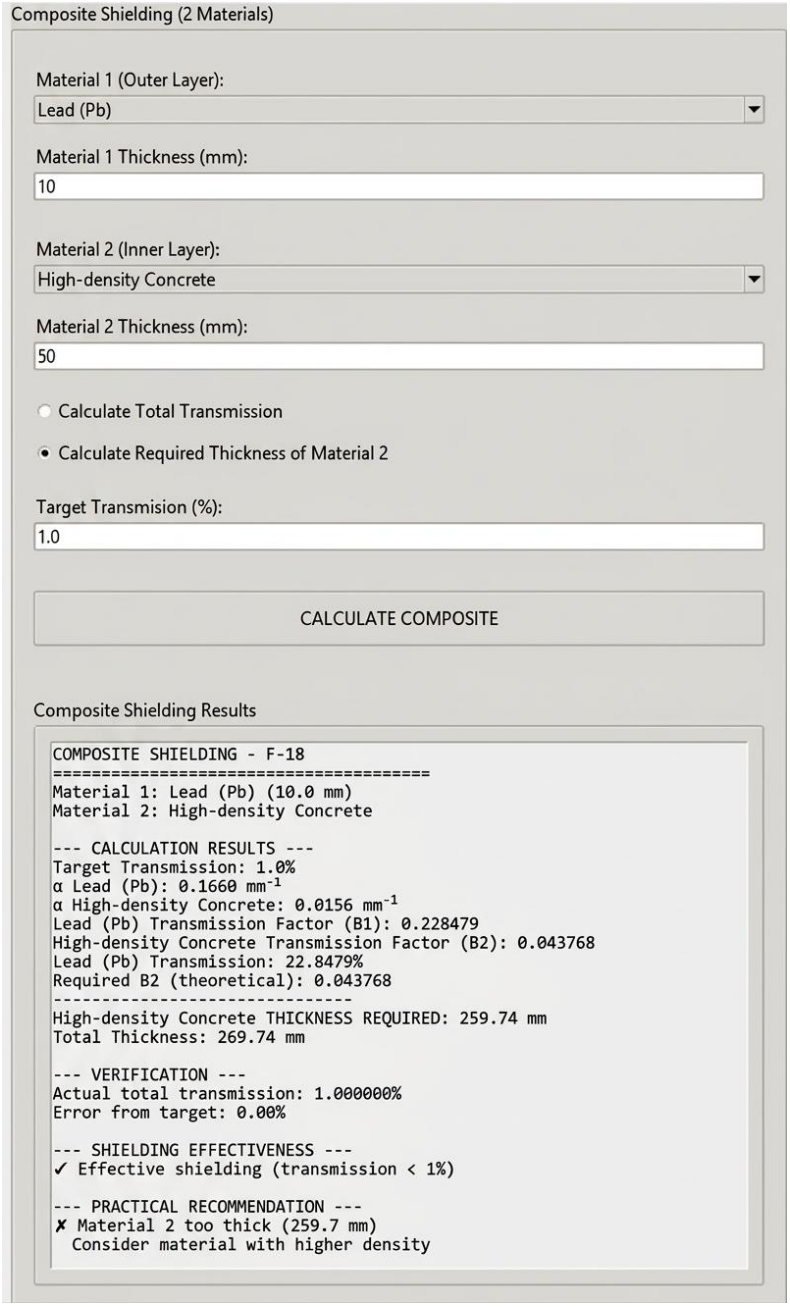


Figure 5. Required shielding thickness for an F-18 source using composite lead and high-density concrete barriers. With Pb fixed at 10 mm ($B_1 = 0.2285$), the calculated concrete thickness is 259.74 mm to achieve 1% total transmission, assuming independent layers.

For the standard F-18 scenario ($D_0 = 0.675$ mSv/week), a total transmission factor of $B_{total} = 0.01$ yields an estimated weekly dose of $0.675 \times 0.01 = 0.00675$ mSv/week, which is below the assumed

design goal of 0.02 mSv/week. The corresponding target transmission factor is B_{target} = 0.02 / 0.675 = 0.0296, indicating that the selected 1% transmission target is more stringent than required for this scenario. However, the calculated concrete thickness (259.7 mm) is substantially greater than the 10 mm lead layer, potentially increasing space requirements and structural loading. These practical implications were not quantitatively evaluated in this study. The calculated concrete thickness for the 1% transmission target is illustrated in Figure 5.

In the current implementation, composite transmission is approximated as the product of the independently calculated transmission factors of the individual shielding layers (Equation 5), using the corresponding Archer fitting parameters for each material. Because the composite transmission is calculated as the product of two independently evaluated transmission factors, the algorithm yields the same total transmission for lead–concrete and concrete–lead configurations, irrespective of the layer sequence.Physically, however, the sequence of high-Z and low-Z materials can affect the photon spectrum incident on the subsequent layer through energy-dependent attenuation, beam hardening, scattering, and secondary photon production (Duan et al., 2025). These effects can influence the buildup factor and are not explicitly represented by the current independent-layer approximation. The results should be regarded as preliminary estimates rather than order-sensitive predictions of actual shielding performance. Validation against Monte Carlo simulations for both lead–concrete and concrete–lead arrangements is therefore required to quantify the effects of material ordering and assess the accuracy of the approximation.

Therefore, to reduce the overall shielding dimensions without compromising attenuation performance, design modifications are recommended. These may include the use of alternative higher-density materials, such as increasing the proportion of lead thickness or substituting the secondary layer with steel, to examine their effect on overall shielding dimensions at the same target transmission. These options were not evaluated in this study, so no conclusion is drawn here about their effect on dimensions, cost, or structural loading.

3.5 Educational Implication

The developed application provides a potential learning resource for medical physics and radiation protection education. The educational relevance of the application is currently based on its computational features and visualization capabilities rather than on empirical evaluation of student learning outcomes. Future work should include structured evaluations involving medical physics students to assess the usability of the application and its potential contribution to conceptual understanding. Its educational potential lies in the computational features, including calculated shielding thicknesses, transmission factors, and attenuation curves for different radionuclides and shielding materials. These features allow users to examine the relationships between photon energy, material properties, shielding thickness, occupancy factors, and the resulting weekly dose under specified calculation scenarios. Related studies in Jurnal Ilmu Fisika have illustrated Monte Carlo dose simulation and radiation-protection measurement comparisons, offering local methodological context without validating the present application (Andani et al., 2026; Ihsan et al., 2026).

Example of learning activity that is possible to do is by a short, guided exercise using a standar scenario and ask students to compare Tc-99m and F-18 in lead. Students first calculate the unshielded weekly doses and the corresponding target transmission factors with a certain design goal. They then run the application to obtain the lead thicknesses and discuss why a difference in the unshielded dose may lead to different thicknesses. Students can also repeat the comparison with other materials and examine the shapes of the curve. This is an example of the intended uses, the effect of the application on learning outcomes was not evaluated in this study and remains to be assessed in future work with structured student evaluations.

The application also enables comparative analysis of single-material and two-layer composite shielding configurations. For example, the calculated results for Tc-99m and F-18 illustrate how differences in photon energy and Archer fitting parameters affect the required shielding thickness. The visualization of attenuation curves provides a means of examining the behavior of the broad-beam transmission model and comparing its predictions with the simple exponential attenuation approach. In the current version, the display does not include simple exponential reference curve, by adding it in next

development of the application, could be supporting teaching activity in which student able to compare broad-beam and simple exponential attenuation approach.

3.6 Limitations and Future Development

Several limitations of this study should be acknowledged. First, the Archer parameters were obtained from Monte Carlo-based fits reported by Oumano et al. (2025) for an infinite barrier, a point source in air, broad-beam geometry, and normal incidence, with transmission factors down to around 10^{-3}. These conditions do not account for patient self-shielding. In addition, different fitting procedures may yield slightly different parameter values for visually similar curves, and the Archer equation was originally developed for continuous X-ray spectra. Because Ga-68 was not simulated in the source study, its parameters were approximated using those for F-18. Second, room scatter from ceilings and floors, which can limit the achievable shielding performance at very low transmission levels, is not modeled in the application (Oumano et al., 2025; Das & Singh, 2022) Recent radiation-transport work also highlights the need to distinguish software verification from physical dosimetry validation (Hill et al., 2024; Ryczkowski et al., 2025).

Third, composite shielding is evaluated by approximating the total transmission as the product of the transmission factors calculated independently for the individual shielding layers. This is invariant to layer order and has not been validated against Monte Carlo simulations (see Effectiveness of Composite Shielding). Future work will include benchmarking the application against Monte Carlo simulations using different material sequences, layer thicknesses, and heterogeneous geometries to quantify the approximation error and assess the influence of layer ordering. Recent modeling of layered shielding materials reinforces the need to account for layer interactions and energy-dependent radiation transport rather than equating independent transmission products with physical validation (Chen et al., 2025; Duan et al., 2025).

Concerning the validity and consistency of the current model, there are several things to check. Firstly, parameter consistency, all the dose rate constants must be referenced to a primary source with a defined dose quantity, and the code must match those values. Second, the comparison with published fractional value layer thicknesses should be reported for all radionuclide-material combinations, and composite approximated should be benchmarked. Lastly, a notification to the user might be added to notify about the default parameter values and that the calculation of Ga-68 relies in the F-18 parameter set when calculated transmission falls below the fitting range and when the input falls outside the range stated in the paper.

Beyond these corrections, additional developments may include incorporating more radionuclides and shielding materials, extending the calculations to distributed sources, enabling export to standard report formats, introducing interactive tutorials and case studies, developing a web-based version of the application that does not require local Python installation. The application currently not integrating national and international radiation protection regulations, any future integration of the regulatory requirements would be developed later.

4. CONCLUSION

An educational desktop application for radiation shielding calculations in nuclear medicine was developed using the Archer broad-beam transmission model and published Monte Carlo-derived fitting parameters. The application provides forward and inverse calculations of shielding thickness and transmission factors for five radionuclides and four shielding materials, incorporating occupancy factors and a selected weekly design goal of 0.02 mSv/week, which is not a regulatory limit. Ga-68 calculations use the F-18 Archer parameters as an unvalidated surrogate. Numerical verification was performed through manual calculations, inverse–forward round-trip consistency checks, and comparisons with published fractional value layer thicknesses for nine radionuclide–material combinations. The composite shielding calculation uses an independent-layer product approximation that has not been independently validated against Monte Carlo simulations and does not account for layer-order effects. Therefore, composite shielding results should be interpreted as preliminary estimates. The application provides an educational tool for exploring forward and inverse shielding calculations, transmission

factors, and attenuation behavior across different materials and shielding configurations. However, its effectiveness in improving student learning outcomes has not been established and requires evaluation in future educational studies.

AUTHOR CONTRIBUTIONS

Conceptualization, Y.P.D.S. and C.C.; methodology, Y.P.D.S.; software, Y.P.D.S.; validation, Y.P.D.S.; formal analysis, C.C.; writing—original draft preparation, C.C.; writing—review and editing, C.C.; visualization, C.C.; supervision, Y.P.D.S. Both authors have read and approved the final version of the manuscript.

FUNDING

This research was funded by the Institute for Research and Community Service (LPPM), Parahyangan Catholic University (UNPAR), through an internal research grant.

DATA AVAILABILITY STATEMENT

The data supporting the findings of this study are available from the corresponding author upon reasonable request.

CONFLICTS OF INTEREST

The authors declare no conflict of interest

ARTIFICIAL INTELLIGENCE (AI) USAGE DECLARATION

During the preparation of this manuscript, the author(s) used ChatGPT (OpenAI) for language editing and assistance in improving the clarity of the manuscript. After using this tool, the author(s) reviewed and edited the output as needed and take full responsibility for the content of the publication.

REFERENCES

Andani, T. S., Oktamuliani, S., Saputro, B., Fendinugroho, Firmansyah, O. A., & Nuraeni, N. (2026). Monte Carlo simulation of depth-dose distribution in medical polymers irradiated by 10 MeV electron beam using PUFFIn. *Jurnal Ilmu Fisika*, 18(2), 210–218. https://doi.org/10.25077/jif.18.2.210-218.2026

Archer, B., Thornby, J., & Bushong, S. (1983). Diagnostic X-ray Shielding Design Based on an Empirical Model of Photon Attenuation. *Health Physics*, *44*(5), 507–517.

Arruzza, E., Chau, M., & Kilgour, A. (2023). Problem-based learning in medical radiation science education: A scoping review. *Radiography*, 29(3), 564–572. https://doi.org/10.1016/j.radi.2023.03.008

AZoM. (2012). AISI A514 Grade A Alloy Steel (UNS K11856). https://www.azom.com/article.aspx?ArticleID=6736 Accessed on October 28, 2026.

Basu, P., Sarangapani, R., & Venkatraman, B. (2019). Gamma ray buildup factors for conventional shielding materials and buildup factors computed for tungsten with a thickness beyond 40 mean free paths. *Applied Radiation and Isotopes*, 154, 108864. https://doi.org/https://doi.org/10.1016/j.apradiso.2019.108864

Bektasoglu, M., & Bayraktar, A. S. (2026). GRASP-X: A user-friendly web-based code to compute various gamma shielding parameters. *Radiation Physics and Chemistry*, 243, 113646. https://doi.org/10.1016/j.radphyschem.2026.113646

Chau, M., & Arruzza, E. S. (2023). Maximising undergraduate medical radiation students' learning experiences using cloud-based computed tomography (CT) software. *Simulation & Gaming*, 54(4). https://doi.org/10.1177/10468781231178491

Chau, M., Arruzza, E., & Johnson, N. (2022). Simulation-based education for medical radiation students: A scoping review. *Journal of Medical Radiation Sciences*, 69(3), 367–381. https://doi.org/https://doi.org/10.1002/jmrs.572

Chen, J., Li, R., Chen, Y., Cao, C., & Liang, J. (2025). POKER: A new point kernel 3D radiation field characterization code with stratified and deep shielding capabilities. *Nuclear Engineering and Technology*, 57(6), 103410. https://doi.org/10.1016/j.net.2024.103410

Cherry, S. R., Sorenson, J. A., & Phelps, M. E. (2012). Physics in Nuclear Medicine. In *Physics in Nuclear Medicine*. https://doi.org/10.2967/jnumed.113.123125

Das, A., & Singh, T. (2022). Development of a new Monte Carlo based transport code to calculate photon exposure build-up factors in various shielding arrangements. *Radiation Physics and Chemistry*, 194, 110028. https://doi.org/https://doi.org/10.1016/j.radphyschem.2022.110028

Dorostkar, M. M., & Rasouli, F. S. (2025). Artificial neural network for optimizing gamma radiation shielding. *Journal of Biomedical Physics and Engineering*, 15(6), 567–574. https://doi.org/10.31661/jbpe.v0i0.2312-1694

Duan, X., Zhao, J., Song, S., Zhou, N., Fan, J., Tian, B., & Du, Y. (2025). Layered structural engineering of Bi2O3/PP and WO3/PP composites for γ-ray shielding in high energy range: anisotropic attenuation mechanisms via Monte Carlo simulation and experiments. *Journal of Materials Research and Technology*, *36*, 10324–10336. https://doi.org/https://doi.org/10.1016/j.jmrt.2025.05.223

Ferrari A,Sala PR,Fasso A, R. J. (2005). a multi-particle transport code. *FLUKA, CERN*.

Ganou, C., Ganos, A., Papatheodorou, S., Metaxas, V., Dimitroukas, C., & Panayiotakis, G. (2023). Radiotherapy Infrastructure Shielding Calculations: software development for shielding calculations in a linear accelerator radiotherapy room. *Radiation Protection Dosimetry*, 199(13), 1357–1366. https://doi.org/10.1093/rpd/ncad189

Gonzales, J. M. G. F., Romallosa-Dean, K. M., Ramo, M. E. S. K. V., & Parami, V. K. (2025). A comparative study on the shielding calculation methods for an optimal shielding design of isolation rooms in a nuclear medicine facility in the Philippines providing I-131 thyroid ablation therapy. *Health Physics*, 129(6), 501–513. https://doi.org/10.1097/HP.0000000000001988

Hansda, M. K., & Mammen, S. (2021). 3DGShield: A new 3D gamma ray shielding code for arbitrary source and shield geometry based on point kernel technique. *Annals of Nuclear Energy*, *159*, 108352. https://doi.org/https://doi.org/10.1016/j.anucene.2021.108352

Hill, M. A., Staut, N., Thompson, J. M., & Verhaegen, F. (2024). Dosimetric validation of SmART-RAD Monte Carlo modelling for x-ray cabinet radiobiology irradiators. *Physics in Medicine & Biology*, 69(9), 095014. https://doi.org/10.1088/1361-6560/ad3720

Hubbell, J. H., & Seltzer, S. M. (1995). *Tables of X-ray mass attenuation coefficients and mass energy-absorption coefficients 1 keV to 20 MeV for elements Z= 1 to 92 and 48 additional substances of dosimetric interest* (No. PB-95-220539/XAB; NISTIR-5632). National Inst. of Standards and Technology-PL, Gaithersburg, MD (United States). Ionizing Radiation Div.

Ihsan, Z. M., Anggraini, M., Sabana, A., Aminudin, M., Urip, T., Jundi, A. F., & Firmansyah, O. A. (2026). Radiation protection intercomparison activity for N-60 and N-80 X-ray beam qualities: Results from SNSU-BSN Indonesia. *Jurnal Ilmu Fisika*, 18(2), 219–229. https://doi.org/10.25077/jif.18.2.219-229.2026

Levart, D., Kalogianni, E., Corcoran, B., Mulholland, N., & Vivian, G. (2019). Radiation precautions for inpatient and outpatient 177Lu-DOTATATE peptide receptor radionuclide therapy of neuroendocrine tumours. *EJNMMI Physics*, *6*(1), 1–12. https://doi.org/10.1186/s40658-019-0243-1

Li, X., Marschall, T. A., Yang, K., & Liu, B. (2024). Radiation shielding transmission data for modern digital radiography. *Medical Physics*, 51(12), 8768–8775. https://doi.org/10.1002/mp.17449

Mann, K. S., & Mann, S. S. (2021). Py-MLBUF: Development of an online-platform for gamma-ray shielding calculations and investigations. *Annals of Nuclear Energy*, 150, 107845. https://doi.org/https://doi.org/10.1016/j.anucene.2020.107845

Manohara, S. R., Hanagodimath, S. M., & Gerward, L. (2011). Energy absorption buildup factors of human organs and tissues at energies and penetration depths relevant for radiotherapy and diagnostics. *Journal of Applied Clinical Medical Physics*, 12(4), 3557. https://doi.org/10.1120/jacmp.v12i4.3557

Marshall, S. K., Kwandee, P., Songphum, N., & Chuaymuang, J. (2025). Comprehensive Simulation-Based Evaluation of Gamma Radiation Shielding Performance of Bismuth Oxide- and Tungsten Oxide-Reinforced Polymer Composites for Nuclear Medicine Occupational Safety. *Polymers*, 17(11), 1–30. https://doi.org/10.3390/polym17111491

Oumano, M., Wendt, R., Botti, J., Busse, N., Hintenlang, D., Leon, S., Little, K., Martin, M., Massoth, R., Matthews, K., Prasad, R., White, S., & Clements, J. (2025a). Shielding resources for four common radiopharmaceuticals utilized for imaging and therapy: Tc-99m, F-18, I-131, and Lu-177. *Journal of Applied Clinical Medical Physics*, 26(5), 1–15. https://doi.org/10.1002/acm2.70084

Paixão, L., Ferreira Fonseca, T. C., & Soares, A. D. (2025). Comprehensive assessment of broad beam transmission factors for nuclear medicine shielding. *Physica Medica: European Journal of Medical Physics*, 130. https://doi.org/10.1016/j.ejmp.2025.104918

Prasada, D. N. Y., & Azzi, A. (2025). Calculation of TVL and HVL for shielding requirements in radiotherapy facilities using Monte Carlo simulation. Buletin Fisika, 26(2). https://doi.org/10.24843/BF.2025.v26.i02.p02

Protection, I. C. on R. (2007). The 2007 Recommendations of the International Commission on Radiological Protection: ICRP Publication 103. *Annals of the ICRP*, 37(2–4), 9–34. https://doi.org/10.1016/j.icrp.2007.10.003

Riveira-Martin, M., Struelens, L., Muñoz Iglesias, J., Schoonjans, W., Tabuenca, O., Nogueiras, J. M., Salvador Gómez, F. J., & López Medina, A. (2023). Radiation exposure assessment of nuclear medicine staff administering [177Lu]Lu-DOTA-TATE with active and passive dosimetry. *EJNMMI Physics*, 10(1), 1–25. https://doi.org/10.1186/s40658-023-00592-1

Ryczkowski, A., Kruszyna-Mochalska, M., Pawałowski, B., Bielęda, G., Jodda, A., Adrich, P., & Piotrowski, T. (2025). Shielding disc backscatter calculations in intraoperative radiotherapy using a Monte Carlo simulation based on the method of energy spectra reconstruction. *Scientific Reports*, 15, 12431. https://doi.org/10.1038/s41598-025-97522-1

Şakar, E., Özpolat, Ö. F., Alım, B., Sayyed, M. I., & Kurudirek, M. (2020). Phy-X / PSD: Development of a user friendly online software for calculation of parameters relevant to radiation shielding and dosimetry. *Radiation Physics and Chemistry*, 166, 108496. https://doi.org/https://doi.org/10.1016/j.radphyschem.2019.108496

Saleh, H. H., Sharaf, J. M., & Abady, R. S. (2021). Gamma-ray buildup factor and radiation absorbed dose enhancement at tissue-bone interfaces. *Applied Radiation and Isotopes*, 167, 109464. https://doi.org/https://doi.org/10.1016/j.apradiso.2020.109464

Salehzahi, F., & Tse, J. (2020). Shielding commissioning factors in nuclear medicine facilities. *Journal of Radiological Protection*, 40(1), 165. https://doi.org/10.1088/1361-6498/ab504e

Shimizu, A., Onda, T., & Sakamoto, Y. (2004). Calculation of gamma-ray buildup factors up to depths of 100 mfp by the method of invariant embedding, (III). *Journal of Nuclear Science and Technology*, 41(4), 413–424. https://doi.org/10.1080/18811248.2004.9715503

Sosa Vera, C., & Andres, P. (2022). Design and development of a web-based application for structural shielding calculation of medical X-ray imaging facilities. *Applied Computing and Informatics*, 18(3–4), 235–244. https://doi.org/10.1016/j.aci.2019.12.002

Sun, P., Xing, L., Yin, L., Chang, Y., Wu, S., Zhong, B., Shen, H., & Ying, Y. (2026). LSPBF: A new open-source large-scale photon buildup factor database. *Radiation Physics and Chemistry*, 245, 113827. https://doi.org/https://doi.org/10.1016/j.radphyschem.2026.113827

Sun, P., Xing, L., Yin, L., Huang, J., Zhong, B., Shen, H., & Ying, Y. (2025). Calculation of gamma-ray buildup factors up to 100 MFP by the Monte Carlo method. *Radiation Physics and Chemistry*, 233, 112696. https://doi.org/10.1016/j.radphyschem.2025.112696

Tarabin, M., & Hisseine, O. A. (2026). PARSO—Particle-packing and radiation shielding optimizer: A user-friendly software tool for fostering the discovery of high-performance radiation-shielding materials. *Radiation Physics and Chemistry*, 114367. https://doi.org/10.1016/j.radphyschem.2026.114367

Wu, J., Wu, Z., Hu, A., Hao, Y., Pu, Y., Zhang, H., Qiu, R., & Li, J. (2025). Optimization progress of large-scale radiation shielding Monte Carlo simulation software based on AIS variance reduction technique system: MCShield. *EPJ Nuclear Sciences and Technologies*, 11. https://doi.org/10.1051/epjn/2024032